Molecules and Cells

Arabidopsis MAP3K16 and Other Salt-Inducible MAP3Ks Regulate ABA Response Redundantly

Seo-wha Choi[1,2], Seul-bee Lee[1,2], Yeon-ju Na[1], Sun-geum Jeung[1], and Soo Young Kim[1,*]

[1]Department of Biotechnology and Kumho Life Science Laboratory, College of Agriculture and Life Sciences, Chonnam National University, Gwangju 61186, Korea, [2]These authors contributed equally to this work.
*Correspondence: sooykim@chonnam.ac.kr
http://dx.doi.org/10.14348/molcells.2017.0002
www.molcells.org

In the Arabidopsis genome, approximately 80 MAP3Ks (mitogen-activated protein kinase kinase kinases) have been identified. However, only a few of them have been characterized, and the functions of most MAP3Ks are largely unknown. In this paper, we report the function of MAP3K16 and several other MAP3Ks, MAP3K14/15/17/18, whose expression is salt-inducible. We prepared *MAP3K16* overexpression (OX) lines and analyzed their phenotypes. The result showed that the transgenic plants were ABA-insensitive during seed germination and cotyledon greening stage but their root growth was ABA-hypersensitive. The OX lines were more susceptible to water-deficit condition at later growth stage in soil. A *MAP3K16* knockout (KO) line, on the other hand, exhibited opposite phenotypes. In similar transgenic analyses, we found that *MAP3K14/15/17/18* OX and KO lines displayed similar phenotypes to those of MA3K16, suggesting the functional redundancy among them. MAP3K16 possesses *in vitro* kinase activity, and we carried out two-hybrid analyses to identify MAP3K16 substrates. Our results indicate that MAP3K16 interacts with MKK3 and the negative regulator of ABA response, ABR1, in yeast. Furthermore, MAP3K16 recombinant protein could phosphorylate MKK3 and ABR1, suggesting that they might be MAP3K16 substrates. Collectively, our results demonstrate that MAP3K16 and MAP3K14/15/17/18 are involved in ABA response, playing negative or positive roles depending on developmental stage and that MAP3K16 may function *via* MKK3 and ABR1.

Keywords: abiotic stress, abscisic acid (ABA), *Arabidopsis thaliana*, MAP kinase, MAP3K16

INTRODUCTION

The plant hormone abscisic acid (ABA) plays important roles in plant growth and development (Finkelstein, 2013). Plants are exposed to various adverse environmental conditions such as drought, high salinity, and extreme temperatures during their life cycle. Under these conditions, ABA level increases, and ABA mediates protective responses to the abiotic stresses (Nambara and Marion-Poll, 2005). For instance, ABA minimizes water loss through transpiration by promoting stomatal closure and, at the same time, inhibiting stomatal opening under water deficit condintion (Kim et al., 2010). It also controls the synthesis of compatible osmolytes and coordinates other responses to protect cells from the damage caused by various stresses (Xiong et al., 2002). Additionally, ABA functions, in general, as a negative regulator of plant growth under the stress conditions (Finkelstein, 2013). It inhibits seed germinaton, seedling establishment and the onset of postgermination growth, and subsequent seedling growth. Cellular ABA level is high also in developing seeds, and it plays a key role in the synthesis of storage components and establishing seed dormancy during seed maturation (Holdsworth et al., 2008). Most of the cellular processes controlled by ABA entail changes in gene expression, and numerous genes are

Received 31 December, 2016; accepted 16 January, 2017; published online 14 March, 2017

eISSN: 0219-1032

known to be regulated by ABA (Fujita et al., 2011).

The molecular components comprising the ABA response pathway have been identified by various genetic and biochemical studies, and the core signaling pathway leading to the ABA-dependent gene expression has been unraveled (Cutler et al., 2010; Yoshida et al., 2015). ABA is perceived by PYR/PYL/RCAR family receptor proteins (Ma et al., 2009; Park et al., 2009). The ABA-bound receptor proteins interact with the members of the clade A subfamily of PP2Cs (e.g, ABI1, ABI2, and HAB1). The PP2Cs are negative regulators of ABA signaling and, in the absence of ABA, inactivate a subset of SnRK2s (e.g., OST1/SnRK2.6/SnRK2E, and SnRK2.2/SnRK2D, and SnRK2.3/SnRK2I) (Fujii and Zhu, 2009; Fujita et al., 2009). The receptor binding to the PP2Cs inhibits the phosphatase activity of PP2Cs, resulting in the activation of the SnRK2s. The activated SnRK2s phosphorylate the ABF/AREB/ABI5 family of bZIP class transcription factors that regulate ABA-responsive gene expression. Thus, the core ABA signaling pathway that leads to the ABA-regulated gene expression consists of PYR/PYL/RCAR-PP2Cs-SnRK2s-ABFs/AREBs/ABI5 (Fujii et al., 2009).

Mitogen-activated protein kinase (MAPK) signaling cascades play diverse roles in eukaryotic cell signaling (Colcombet and Hirt, 2008; Rodriguez et al., 2010). A typical MAPK cascade consists of three MAP kinases: MAP kinase kinase kinase (MAPKKK/MAP3K), MAPkinase kinase (MAPKK/MAP2K), and MAP kinase (MAPK). The signaling module, which is universal among eukaryotic kingdom, is activated by various internal or external stimuli, such as mitogen, hormones, developmental signal, pathogen, and abiotic stresses. The kinases comprising the module is sequentially activated by a relay of phosphorylation. A MAP3K, which is activated by a specific stimulus or stimuli, phosphorylate MAP2K, which, in turn, phosphorylate MAPK. The activated MAPKs phosphorylate downstream targets to modify their activities.

In the Arabidopsis genome, approximately 80 MAP3Ks, 10 MAP2Ks, and 20 MAPKs have been identified (Colcombet and Hirt, 2008). Numerous studies have been carried out to determine the functions of individual MAPKs, especially those of MAP2Ks and MAPKs. The studies show that they are involved in various cellular processes, such as plant development, hormone responses, disease resistance, and abiotic stress responses (Colcombet and Hirt 2008; Rodriguez et al., 2010). In several cases, the entire signaling cascades comprised of MAP3K-MAP2K-MAPK have been delineated. For instance, the MEKK1-MKK2-MPK4/6 modules are involved in salt and cold response (Teige et al., 2004), the MEKK1-MKK4/5-MPK3/6 modules function in innnate immunity (Asai et al., 2002), and the YODA-MKK4/5-MPK3/6 modules regulate the stomatal development (Lampard et al., 2009).

Some MAPKs are involved in ABA response (Liu, 2012). The MKK1-MPK6 module mediates ABA response during seed germination by regulating *CAT1* expression and glucose-induced ABA level (Xing et al., 2008; 2009). MPK9 and MPK12 positively regulate both ABA- and MeJA-dependent guard cell signaling (Jammes et al., 2009; Khokon et al., 2015). Additionally, a large number of MAPKs in Arabidopsis and other plant species are known to be induced or activated by ABA and abiotic stresses (Danquah et al., 2014). Although the role of individual MAPKs and their signaling module in ABA signaling have been established for a number of cases, specific functions of MAPKs remain largely unknown. This is especially so in the case of MAP3Ks. MAP3Ks constitute the largest MAPK family (i.e., approximately 80 members), but only a few of them have been charaterized functionally (Rodriguez et al., 2010). MEKK1 regulates innnate immunity and abiotic stress responses, as mentioned above, and YODA controls stomatal patterning (Lampard et al., 2009; Teige et al., 2004). ANP1 and its homologs, on the other hand, positively regulate cytokinesis (Takahashi et al., 2010). Most recently, MAP3K17/18 have been reported to mediate ABA response *via* the MKK3-MPK1/2/7/14 pathway (Danquah et al., 2015; Matsuoka et al., 2015). MAP3K17/18 is activated by ABA, and their mutants are ABA-hypersensitive. Mitula et al. (2015) further reported that MAP3K18 activity is regulated by ABI1.

We are interested in the roles of MAP3Ks in ABA and/or abiotic stress signaling and set out to investigate the ABA-associated functions of several MAP3Ks. We chose MAP3K16 and other related MAP3Ks for our study. MAP3K16 is one of the several salt-inducible MAP3Ks, together with MAP3K14, MAP3K15, MAP3K17, and MAP3K18 (i.e., MAP3K14/15/17/18). MAP3K17 and MAP3K18 are also ABA-inducible. As a first step toward their functional analysis, we investigated whether MAP3K16 and the related MAP3Ks, MAP3K14/15/17/18, are involved in ABA response. In this paper, we show that MAP3K16 regulates a subset of ABA response and present the data suggesting its possible substrates. Our results further indicate that MAP3K14/15/17/18 play similar roles in ABA response.

MATERIALS AND METHODS

Plant growth and RNA isolation

Plants (*Arabidopsis thaliana*, ecotype L*er* and Col-0) were grown at 22°C under long day condition (16 h light/8 h dark cycle). For aseptic growth, seeds were placed on MS medium supplemented with 1% sucrose and solidified with 0.8% agar. If necessary, the MS medium was supplemented with ABA, salt or other supplements as indicated in the Figure legends. Seeds were placed at 4°C for 3-5 days in the dark to break residual dormancy before being transferred to normal growth temperature. For soil growth, seeds were sown on 1:1:1 mixture of vermiculite, perlite, and peat moss, and, after stratification, placed at normal growth condition. Plants were watered once a week by immersing pots in 0.1% Hyponex (Hyponex Co., USA) solution.

RNA isolation, semi-quantitative RT-PCR, and real-time RT-PCR were performed described previously (Lee et al., 2015). Briefly, RNA was isolated employing the RNeasy plant mini kit (Qiagen) and treated with DNase I to remove contaminating DNA. For RT-PCR, the first strand cDNA was synthesized using Superscript III (Invitrogen), and qRT-PCR was carried out in a Bio-Rad CFX96 real-time PCR system using the primers shown in the Supplementary Table S2. *UBC9* (At4g27960) (Czechowski et al., 2005) was used as a reference gene.

Generation of transgenic plants and phenotype analysis

The *promoter-GUS* construct was prepared by amplifying a 2.2 kb 5′ flanking sequence of the *MAP3K16* gene and cloning it into the Sal I/Bam HI sites of pBI101.2 (Jefferson et al., 1987), using the primers shown in Supplementary Table S2. For overexpression (OX) lines, entire coding region of each *MAP3K* was amplified using the primer sets shown in the Supplementary Table S2, and after digestion with appropriate enzymes, cloned into pBI121 (Jefferson et al., 1987).

Transformation of Arabidopsis was performed according to Bechtold and Pelletier (Bechtold and Pelletier, 1998). For the promoter analysis, T3 homozygous lines were employed in histochemical GUS staining. For OX lines, more than 100 T1 transgenic lines were selected for each construct, and T3 generation homozygous lines were recovered from T2 generation lines segregating with 3:1 ratio of Kan^R and Kan^S seeds. Final phenotype analyses were carried out using T4 generation seeds of representative lines after preliminary analyses of T3 generation homozygous lines. The knockout (KO) mutant, *map3k16* (SALK_003255C), was acquired from the Arabidopsis stock center. Seeds of progeny were collected from individual plants, and, after selecting homozygous plants, T-DNA insertion was confirmed first by PCR using primers flanking the insertion site and then by sequencing of the genomic DNA fragment flanking the right border. Phenotype analyses were performed using the seeds amplified from the confirmed lines. For the analyses of *MAP3K15/17/18* KO lines described in the Supplementary Table S1, following seed stocks were acquired form the Arabidopsis stock center: SALK102721C (*map3k15*), SALK080309C (*map3k17*), and CS309974 (*map3k18*). The T-DNA insertion in the respective annotated sites in the mutants were confirmed in the same way as for the *map3k16* mutant identification.

Phenotype analyses were carried out as described before (Kang et al., 2002; Lee et al., 2015). Germination and cotyledon greening efficiency were scored as described in the Figure legends, using seeds harvested at the same time. For drought test, same number of wild type and transgenic plants (20 each) were grown in the same tray to minimize possible position effect. The test was repeated several times in multiplicates and representative results are presented.

Yeast two-hybrid assay and other interaction study

Yeast two-hybrid assays were performed as described before (Choi et al., 2005; Lee et al., 2009). To prepare bait constructs, insert fragments were amplified using the primers shown in the Supplementary Table S2 and cloned into the pPC62LexA vector (Lee et al., 2009). The prey constructs were prepared by cloning the individual amplified fragments into pYESTrp2 (Invitrogen). Bait constructs were individually introduced into the reporter yeast L40 (*MATα, his3Δ200, trp1-901, leu2-3112, ade2, LYS2::[LexAop(x4)-HIS3], URA3::LexAop[x8]-LacZ,* GAL4) (Invitrogen; Carlsbad, Calif) by transformation, and relevant prey constructs were subsequently introduced. To test interactions, yeast transformants were grown on SC-His medium, and the *LacZ* activity was assayed by X-gal overlay assay (Duttweiler, 1996) or by the liquid assay using O-nitrophenyl-β-D-galactopyranoside (ONPG) as a substrate.

Pulldown assays were performed as described before (Choi et al., 2005) with minor modification. For ABR1, maltose-binding protein (MBP) was used as a negative control, and glutathione S-transferase (GST) was used as a negative control for MKKs (see below). Approximately 5 μg of fusion proteins, 30 μl of MBP (ABR1) or GST (MKKs) resin (50% slurry), and 20 μl of *in vitro* translation products were used in each binding reaction. For *in vitro* translation, the *MAP3K16* coding region was cloned into the Eco RI/Xho I sites of pCITE-4a (Novagen; USA). *In vitro* translation was carried out employing the TNT *in vitro* translation kit (Promega; Madison, WI) according to the supplier's instruction. BiFC was performed according to Walter et al. (2004). *MAP3K16*, *ABR1*, and *MKK3* were individually cloned into pSPYNE-35S and pSPYCE-35S, respectively. Pairwise combinations of the constructs (i.e., two pairs for *ABR1* and two pairs for *MKK3*) were then used to infiltrate tobacco leaves (*N. benthamiana*). Because epifluorescence signals were very weak, protoplasts were prepared (Yoo et al., 2007) from the tobacco leaves 3-5 days after infiltration and observed under the microscope (Olympus BX51). Fluorescence signals were detected from the pairs shown in Figs. 6C and 7C.

Preparation of recombinant proteins and *in vitro* kinase assay

MAP3K16 recombinant proteins were prepared employing the pMAL system (NEB) with the modification described previously (Lee et al., 2015). The entire coding region (amino acids 1-443) or the kinase domain (amino acids 1-263) were amplified and cloned into the Sal I/Eco RI sites of pMAL-c5X with a 6X His-tag. Protein induction and protein purification were carried out according to the supplier's instruction, and the proteins were further purified employing the Ni-NTA resin (Qiagen). ABR1 recombinant protein was prepared in a similar way. The entire *ABR1* coding region (amino acids 1-391) was amplified and cloned in to the Nde I/Sal I sites of pMAL-c5X (NEB), and protein was purified by employing amylose resin followed by Ni-NTA resin. Primer sequences are shown in the Supplementary Table S2. MKK3 and other MKK (Supplementary Figs. S4 and S6) recombinant protein were prepared using a GST-fusion vector, pColdIII-GST-His. The vector was constructed by cloning the GST coding region into Nde I/Kpn I sites of the pColdIII vector (Takara) and then by inserting a 6X His-tag next to the Xba I site. The entire coding region of each *MKK* was amplified using the primer set in the Supplementary Table S2 and cloned into pColdIII-GST-His. Protein induction and purification was carried out according to the GST Gene Fusion System manual (GE Healthcare), and then further purified on Ni-NTA resin.

Kinase assays were carried out as described (Choi et al., 2005; Lee et al., 2015). Briefly, approximately 0.5-1 μg of MAP3K16 recombinant proteins were incubated with similar amounts of substrates in a buffer (25 mM Tris-HCl, pH7.5, 10mM $MgCl_2$, 10 μM ATP) containing 2 μCi of γ-^{32}P for 30 min at 30°C. After the reaction, the reaction mixtures were separated by SDS-PAGE, and gels were stained with Coomassie Brilliant Blue R, dried and autoradiographed.

Table 1. ABA- and stress-induced expression of *MAP3K14/15/16/17/18*[1]

MAP3Ks	Gene ID	ABA	Salt (NaCl)	Mannitol	Cold[2]	Untreated[3] (Rosette/Root)
MAP3K14	At2g30040	1.28 ± 0.21	6.04 ± 0.31	4.54 ± 0.40	0.66 ± 0.11	29.25/189.91
MAP3K15	At5g55090	1.35 ± 0.05	11.71 ± 2.69	1.88 ± 0.18	0.38 ± 0.05	1.25/7.8
MAP3K16	At4g26890	2.89 ± 0.25	11.72 ± 0.98	2.98 ± 0.26	0.17 ± 0.02	8.21/29.4
MAP3K17	At2g32510	11.47 ± 1.58	62.36 ± 0.25	32.60 ± 0.70	0.66 ± 0.30	19.83/33.43
MAP3K18	At1g05100	68.76 ± 6.95	333.72 ± 54.23	413.35 ± 27.02	1.43 ± 2.03	2.06/3.36

[1]Seedlings were treated with 1/4 MS or 1/4MS containing 100 μM ABA, 250 mM NaCl, or 600 mM mannitol for 4 h before RNA isolation. Experiments were done in triplicates, and the numbers indicate relative expression levels compared with those of ¼ MS. *UBC9* (At4g27960) was used as a reference gene.
[2]Relative expression level compared with the expression level in untreated plants. Seedlings were placed at 4°C for 24 h before RNA isolation.
[3]Expression values are from e-FP Browser (http://bar.utoronto.ca/efp/cgi-bin/efpWeb.cgi)

RESULTS

Expression patterns of Arabidopsis *MAP3K14-18*

To examine the stress-induction pattern of *MAP3K16* expression, we conducted real-time RT-PCR using RNA isolated from seedlings. *MAP3K16* transcript level was increased 12-fold by salt and 3-fold by mannitol (Table 1). Similar induction levels were observed with *MAP3K15*. The salt induction levels of *MAP3K17* and *MAP3K18* were much higher, 62-fold and 333-fold, respectively. In addition, the expression of the two *MAP3K* genes was highly induced by mannitol (33-fold and 413-fold, respectively) and ABA (11-fold and 69-fold, respectively). The induction levels of *MAP3K14* expression was relatively lower (i.e., 5-6 fold by high salt and high osmolarity) (Table 1). However, the basal level of *MAP3K14* expression (i.e., the expression level under normal growth condition) is higher than other *MAP3Ks*, and thus, its expression level after induction is comparable to those of other *MAP3Ks*.

We investigated the expression pattern of *MAP3K16* further by determining its tissue-specific expression pattern. Semi-quantitative RT-PCR (Fig. 1A) showed that *MAP3K16* is expressed in leaves, roots, flowers, and siliques. The transcript level in leaves was lower than in other tissues. To determine temporal and spatial expression patterns, transgenic plants harboring a 2.2.kb *promoter-GUS* reporter construct were prepared, and the promoter activity was assayed by histochemical GUS staining. Figure 1B shows that GUS activity was observed in young, emerging leaves (panel a) and lateral roots of seedlings (panel b). In mature plants, GUS activity was observed in lateral roots (Fig. 1B, b), anthers, and stigma (Fig. 1B, c). Embryos also exhibited GUS activity (Fig. 1B, d).

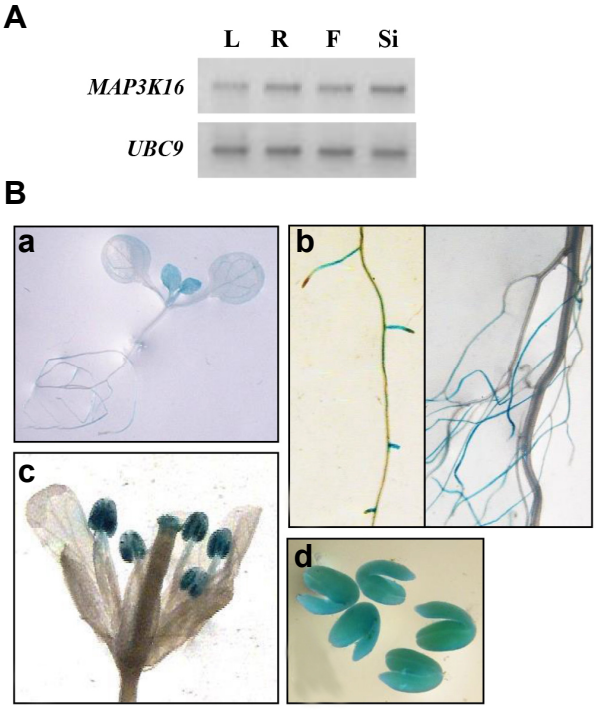

Fig. 1. Expression pattern of *MAP3K16*. (A) Tissue-specific expression pattern of *MAP3K16*. Transcript levels were determined by semi-quantitative RT-PCR using RNA isolated from leaves (L), roots (R), flowers (F), and siliques (Si). (B) Tissue-specific expression pattern of *MAP3K* was determine by histochemical GUS staining of the transgenic plants harboring a 2.2 kb promoter-*GUS* construct. a, 8-day-old seedling. b, Roots of 8-day-old (left) and 39-day-old (right) plants. c, flowers. d, mature embryos.

MAP3K16 OX lines are partially ABA-insensitive

To investigate the *in vivo* function of MAP3K16, we generated its overexpression (OX) lines. The coding region of *MAP3K16* was fused to the constitutive *35S* promoter in pBI121 (Jefferson et al., 1987), and transgenic plants were prepared using the construct. Thirteen homozygous lines were recovered, and, after preliminary analysis, three representative lines were chosen for phenotype analysis (Fig. 2A).

Plants overexpressing *MAP3K16* grew normally, except that they grew faster than wild type plants and, therefore, have a tendency to reach flowering stage slightly earlier (Supplementary Fig. S1). To assess the effect of *MAP3K16* overexpression on ABA response, we examined the ABA-

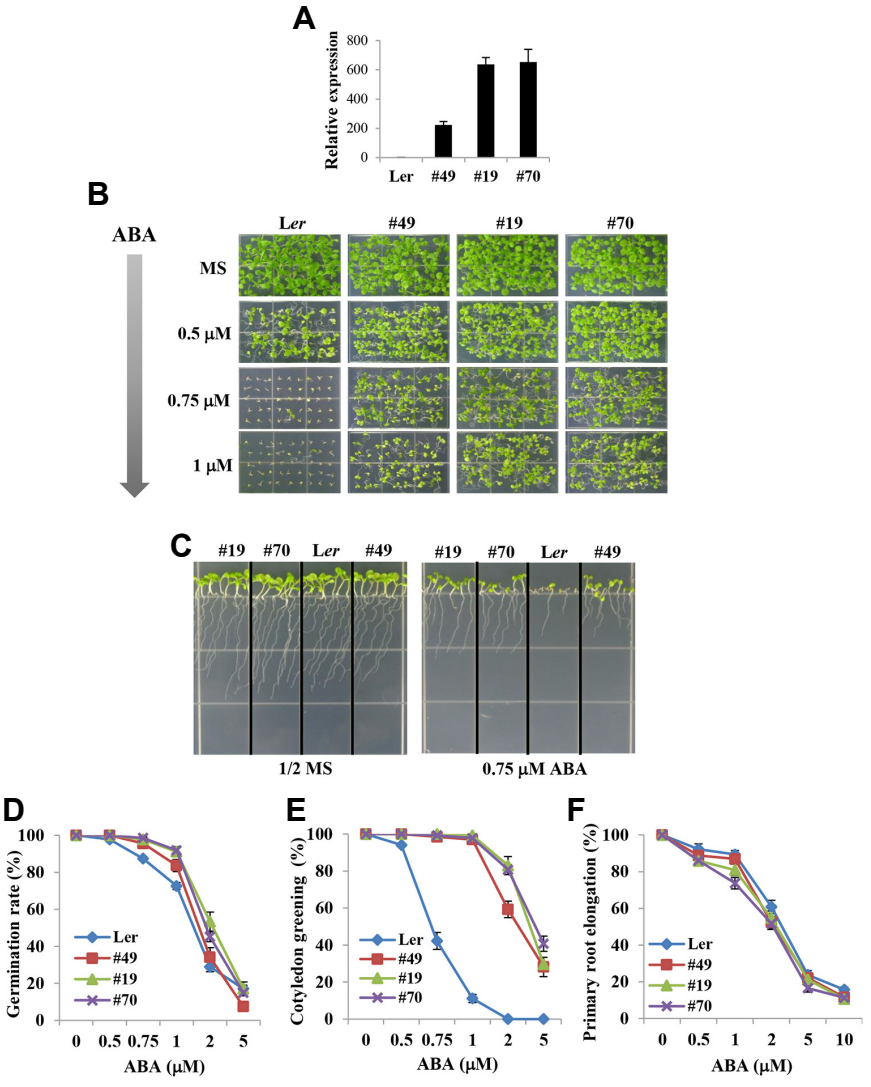

Fig. 2. ABA sensitivity of *MAP3K16* OX lines. (A) Expression levels of *MAP3K16* in the transgenic lines determined by real-time RT-PCR. The error bars denote standard errors (B), (C) ABA sensitivity of seedling growth. Seeds were plated on MS media containing various concentrations of ABA and, after stratification, allowed to germinate and grow for 11 days in horizontal position (B) or 7 days in vertical position (C). (D) ABA sensitivity of seed germination. Mature, dry seeds were plated after stratification on MS medium containing various concentrations of ABA, and germination (radicle protrusion) rates were scored 2 days after plating. Experiments were performed in triplicates (n = 45 each), and the error bars indicate standard errors. (E) ABA sensitivity of cotyledon greening. Seeds were plated, and seedlings with green cotyledons were counted 11 days after plating. Each data point represents the percentage of seedlings with green cotyledons, and the error bars indicate standard errors (triplicates, n = 45 each). (F) ABA sensitivity of root growth. Seeds were germinated and grown for 3 days on ABA-free MS medium, transferred to ABA-containing media, and root elongation was measured 5 days after the transfer. Each data point represents the relative elongation rate compared with the control rate on ABA-free medium. Experiments were done in quintuplicates (n = 5 each), and the error bars denote standard errors.

and stress-associated phenotypes of the OX lines. The most notable phenotype was the partial insensitivity to ABA during early seedling growth stage (Figs. 2B and 2C). When wild type seeds were germinated and grown on the media containing various concentrations of ABA, inhibitory effect of ABA was evident, and the postgermination growth (i.e., shoot and root growth) of wild type seedlings was severely inhibited when ABA concentration was greater than 0.75 μM. ABA inhibition of seedling growth was also observed with the *MAP3K16* OX lines. However, the transgenic plants grew much more efficiently than the wild type plants, suggesting that they were less sensitive to ABA inhibition. To assess the effects of *MAP3K16* overexpression in more detail, we determined the ABA sensitivity during three different stages of early seedling growth: Germination, cotyledon greening/expansion, and primary root elongation. Figure 2D shows that the relative germination rates of transgenic seeds in the presence of ABA were higher than the wild type rates, although the differences were not great. Cotyledon greening/expansion efficiencies of the transgenic seedlings were much higher compared with those of the wild type plants (Fig. 2E). On the other hand, primary root elongation of the transgenic seedlings was more severely affected by ABA than wild type seedlings, although the degree of difference was very low (Fig. 2F). Collectively, the data indicate that ABA sensitivity of the *MAP3K16* OX lines was dependent on developmental stage and that the most prominent growth-related phenotype was the ABA insensitivity during the postgermination seedling establishment (i.e., cotyledon greening) stage.

Stress responses of *MAP3K16* OX lines

Because *MAP3K16* expression is induced by high salt, we also investigated the salt sensitivity of the *MAP3K16* OX lines. The result (Figs. 3A-3C) showed that both germination and cotyledon greening of the transgenic plants were less sensi-

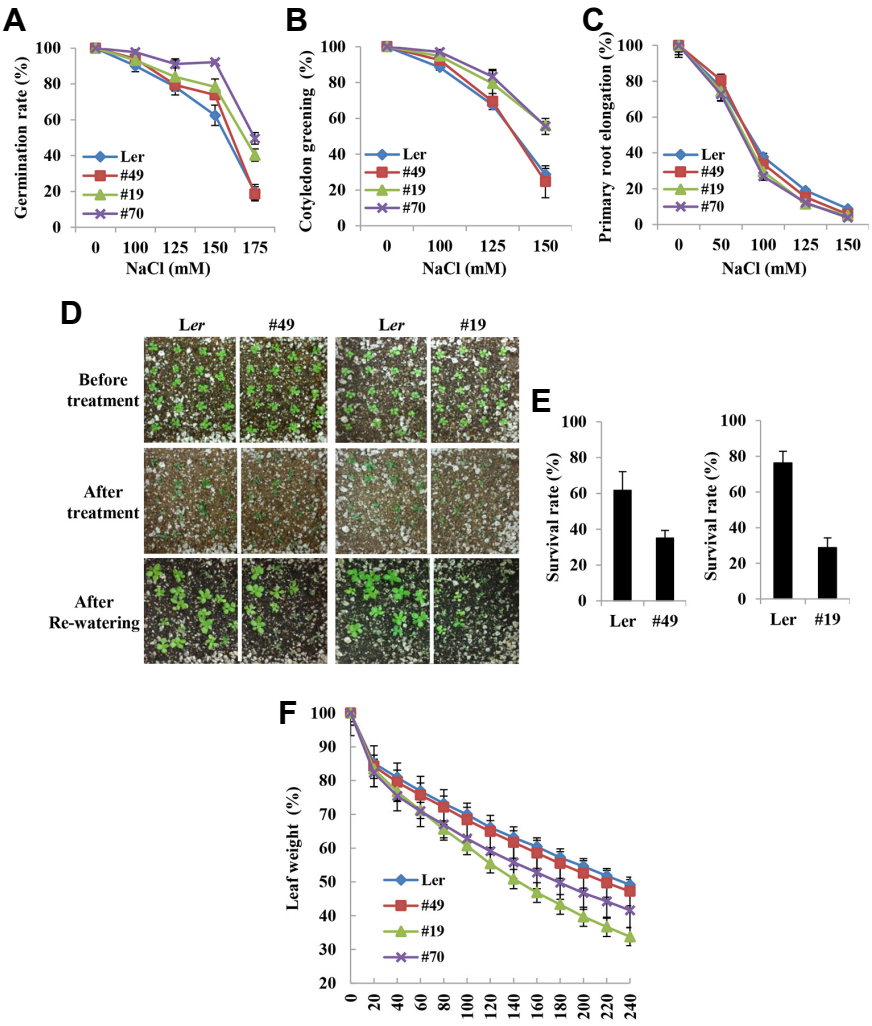

Fig. 3. Stress responses of *MAP3K16* OX lines. (A) Salt sensitivity of seed germination. Seeds were plated after stratification on media containing various concentrations of NaCl, and germination (radicle protrusion) was scores 3 days after the plating. Experiments were done in triplicates (n = 45 each), and the error bars denote standard errors. (B) Salt sensitivity of cotyledon greening. Seeds were plated as in (A), and seedlings with green cotyledons were counted 5 days after the plating. Each data point represents the percentage of seedlings with green cotyledons relative to the control rate on salt-free MS medium. Experiments were done in triplicates (n = 45 each), and the error bars denote standard errors. (C) Salt sensitivity of root growth. Seeds were germinated and grown for 3 days on salt-free MS medium, transferred to media containing NaCl, and root elongation was measured 5 days after the transfer. Each data point represents the relative elongation rate compared with the control rate on ABA-free medium. Experiments were done in quintuplicates (n = 5 each), and the error bars indicate standard errors. (D) Drought tolerance of *MA3K16* OX lines. Plants were grown in soil for 7 days, withheld from water for 12 days, and then re-watered. The bottom panels show plants 2 days after the recovery. To minimize experimental variations, wild type and transgenic plants were grown in the same tray. (E) Survival rates of plants in (D) are presented. Experiments were done in triplicate (#49) (n = 20 each) or quadruplicate (#19) (n = 20 each). (F) Transpiration rates of wild type and *MAP3K16* OX lines. Leaves of the same developmental stage (i.e., 5th and 6th true leaves from 20 day-old plants) were detached and weighed at 20 min interval after the detachment. The data represent relative (percentage) weight compared with the initial weight after the detachment. Experiments were done in triplicates (n = 15 each), and the error bars indicate standard errors.

tive to salt than wild type plants. The partial insensitivity to high salt was observed only at the germination/cotyledon greening stage, and no significant phenotypic changes were observed at later growth stages in salt-containing media (data not shown). The root elongation rates in the presence of salt were similar to the wild type rates, suggesting that the salt sensitivity of primary root elongation was not significantly affected in the *MAP3K16* OX lines.

ABA plays a pivotal role in mediating water-deficit response. Thus, the reduced ABA sensitivity during early seedling growth suggested that the *MAP3K16* OX lines might exhibit altered water-deficit response, presumably reduced tolerance. To test the possibility, we determined the survival rates of the transgenic plants under water-deficit condition. Figures 3D and 3E show that the survival rates of the transgenic lines in soil were lower than the wild type rates. We also determined the transpiration rates of the plants to gain information about the possible mechanism of the reduced tolerance to water-deficit. Figure 3F shows that detached leaves of the *MAP3K16* OX lines lost water faster than the wild type leaves. Thus, our result indicates that the water loss rates of the transgenic leaves were higher.

Phenotypes of a *MAP3K16* knockout mutant

To further investigate the function of MAP3K16, we acquired its knockout (KO) line, *map3k16*, (Figs. 4A and 4B) and examined its ABA sensitivity (Figs. 4C-4E). Figure 4D shows that the germination rates of the *map3k16* seeds were more severely affected than the wild type seeds in the presence of various concentrations of ABA. Similarly, the

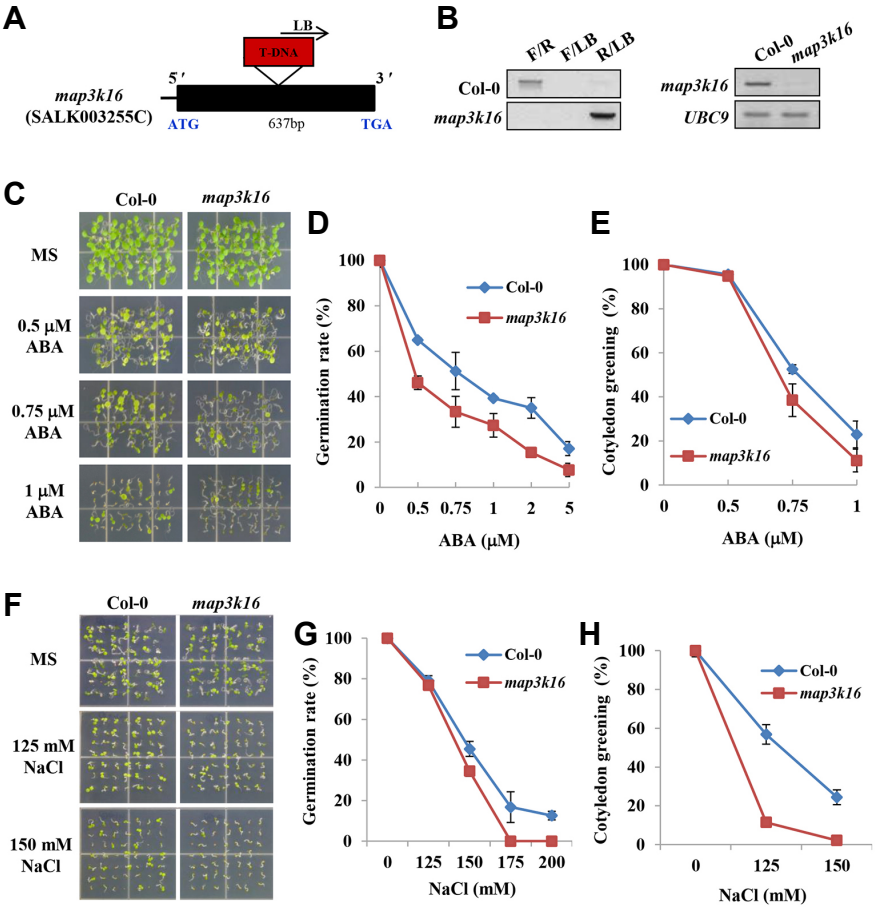

Fig. 4. ABA and salt sensitivity of *MAP3K16* KO line. (A) Schematic presentation of T-DNA insertion site in the *map3k16* mutant. (B) Left, Disruption of the *MAP3K16* gene was confirmed by PCR, using forward (F) and reverse (R) primer set (Supplementary Table S2). Right, Semi-quantitative RT-PCR to confirm the null expression of *MAP3K16*. (C) Growth of the *map3k16* plants on media containing ABA. Plants were grown for 6 days after plating. (D), (E) Seeds were plated in media containing various concentration of ABA, and germination (radicle protrusion) and cotyledon greening were scored one day and 5 days, respectively, after the plating. Experiments were done in triplicates (n = 45 each), and the error bars denote standard errors. (F) Growth of the *map3k16* plants on media containing NaCl. Plants grown for 4 days after plating are shown. (G), (H) Seeds were plated in media containing various concentration of NaCl, and germination and cotyledon greening were scored two days and three days, respectively, after the plating. Experiments were done in triplicates (n = 45 each), and the error bars represent standard errors. The error bars for *map3k16* in (G) and (H) are smaller than the data point symbols.

efficiency of cotyledon greening was also more severely affected by ABA than wild type seedlings (Fig. 4E). Thus, the *map3k16* mutant exhibited ABA-hypersensitive phenotypes during germination and cotyledon greening stage, although the degree of hypersensitivity was relatively low. In addition, the *map3k16* mutant was hypersensitive to high salt during germination and cotyledon greening (Figs. 4F-4H). Overall, our results indicate that the *map3k16* mutant displayed weak ABA-hypersensitive phenotypes, whereas its OX lines exhibited partial ABA insensitivity during early seedling growth (i.e., germination and cotyledon greening/expansion stage).

Phenotypes of other *MAP3K* OX and KO lines

As mentioned earlier, *MAP3K14/15/17/18* are similar to *MAP3K16* in their ABA- and stress-induced expression patterns (Table 1) and are homologous to MAP3K16 to various degrees (i.e., 35 to 64% amino acid sequence identity, Supplementary Fig. S2A). To address whether they also function in ABA and stress responses, we prepared their OX lines and analyzed their phenotypes (Fig. 5).

The plants overexpressing each of *MAP3K14/15/17/18* grew normally except that, like the *MAP3K16* OX line plants, they reached bolting stage slightly earlier than wild type plants (Supplementary Fig. S2B). We first determined the ABA sensitivity of the *MAP3K14* OX lines. Figures 5A-5C show that the transgenic plants were partially insensitive to ABA during early seedling growth stage. Similarly, the OX lines of *MAP3K15/17/18* were partially insensitive to ABA during the same growth stage (Figs. 5D-5L). We next investigated the drought tolerance of the OX lines by scoring the survival rates of seedlings under water-deficit condition. The result showed that the OX lines were more susceptible to water stress than wild type seedlings (Supplementary Fig. S3). Additionally, we acquired and analyzed *MAP3K15/17/18* KO mutants (see Materials and Methods) and found that they displayed similar phenotypes to those of the *map3k16* mutant (summarized in Supplementary Table S1). Collectively, our data indicate that the OX and KO phenotypes of *MAP3K14/15/17/18* are similar to those of *MAP3K16*.

MAP3K16-interacting proteins

MAP3K16 and MAP3K14/15/17/18 belong to the MAP3K family proteins (Ichimura et al., 2002). Because MAP3Ks are components of the MAP kinase module consisted of MAP3K-MAP2K-MAPK, we addressed whether the MAP3Ks

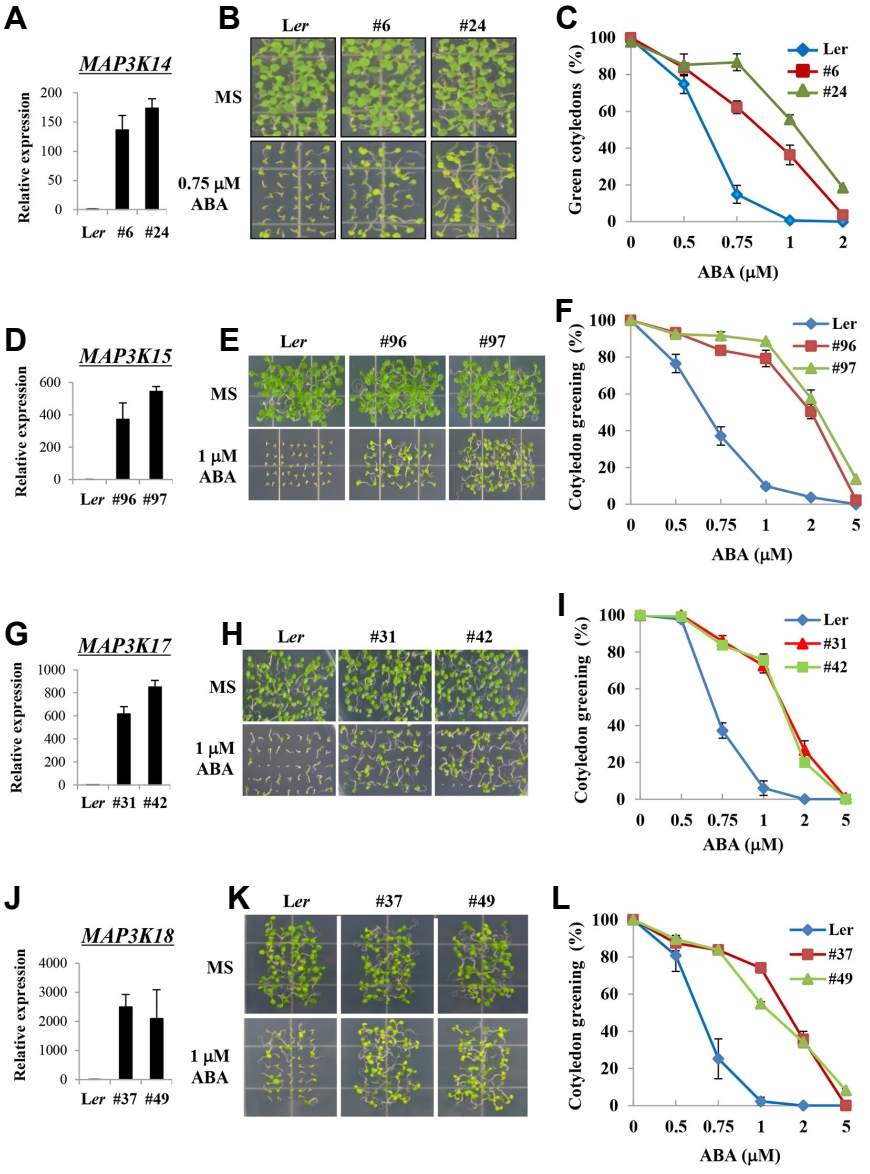

Fig. 5. ABA sensitivity of *MAP3K14/15/17/18* OX lines. (A), (D), (G), (J) Expression levels of *MAP3K14/15/17/18*, respectively, in transgenic lines determined by real-time RT-PCR. Experiments were done in duplicates, and the error bars represent standard errors. (B), (E), (H), (K) Seedlings of *MAP3K14/15/17/18* OX lines grown for 7-9 days after plating on media containing ABA as indicated. (C), (F), (I), (L) Cotyledon greening of the *MAP3K14/15/17/18* OX line seedlings. Each data point represents the percentage of seedlings with green cotyledons counted 5 days (C, F, I) or 7 (L) days after plating. Experiments were done in triplicates (n = 45 each), and the error bars indicate standard errors.

could interact with MAP2Ks by carrying out yeast two-hybrid assays. Bait constructs containing each of the MAP3Ks were prepared, and their interactions with MKKs were examined. The result (Fig. 6) showed that MAP3K16 interacted with MKK3 (Fig. 6A). The interaction was relatively weak (Fig. 6B), but it was consistently detected not only in the two-hybrid assay but also in GST pulldown assay and in bimolecular fluorescence complementation (BiFC) assay. In the pulldown assay (Supplementary Fig. S4), *in vitro* translated MAP3K16 was preferentially retained by MKK3. In the BiFC assay (Fig. 6C), fluorescence signals, which were distributed throughout the cell, were detected in tobacco cells infiltrated with *Agrobacteria* containing the YFP^N-MAP3K16 and the YFP^C-MKK3 construct. Interactions with MKK2/4/5 were also observed occasionally. However, the interactions with these MKKs were very weak (Fig. 6B) and inconsistent, i.e., the results of our interaction assays varied from experiment to experiment (e.g., compare Fig. 6A and Supplementary Fig. S4). Among other MAP3K-MKK pairs, we detected a strong interaction between MAP3K17 and MKK3 (Supplementary Fig. S5).

It is possible that MAP3K16 may interact with proteins other than MKKs. To address the possibility, we performed yeast two-hybrid screening employing the full-length MAP3K16 as bait. We screened approximately 4.5 million yeast transformants obtained with a cDNA expression library prepared from salt- and ABA-treated seedling RNAs (Choi et al., 2000). Several putative positive clones, including APUM10 (At1g35750), CAD7 (At4g37980), ABR1 (At5g64750), and GDA1 (At4g19180), were isolated from the screen. Among the isolates, we chose ABR1 for further analysis, because it is known to be a negative regulator of ABA response (Pandey et al., 2005). As shown in Fig. 7A, ABR1 interacted with the full-length MAP3K16, and it also

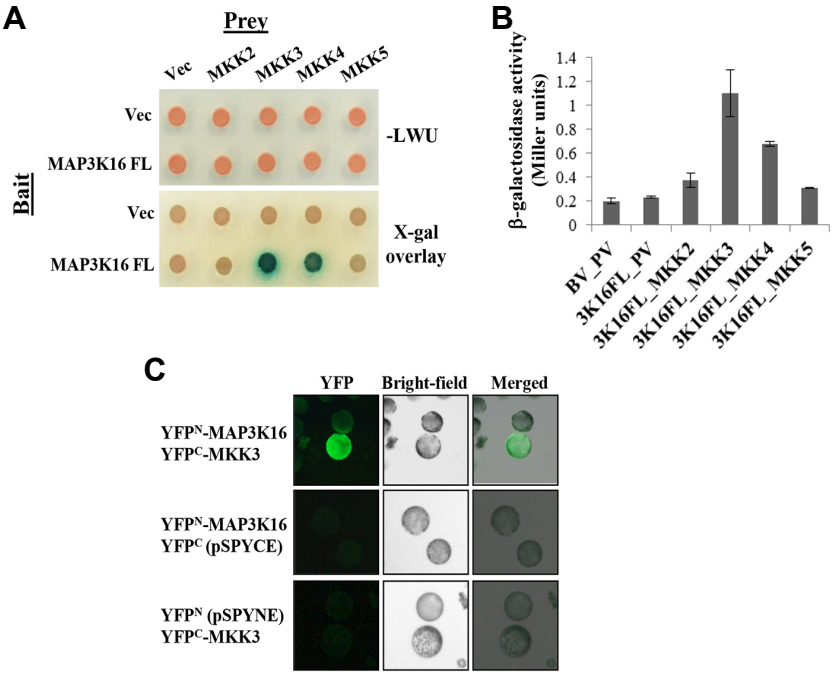

Fig. 6. Interaction of MAP3K16 with MKKs. (A) Interactions between MAP3K16 and MKK2/3/4/5 were examined by two-hybrid assay. Full-length MA3K16 was employed as bait, and MKKs were employed as prey. Yeast transformants were grown on SC-LWU plates, and the *LacZ* reporter activity was determined by X-gal overlay assay. (B) Liquid β-galactosidase assay. The *LacZ* reporter activity was determined by liquid assay using *O*-nitrophenyl-β-D-galactopyrano-side (ONPG) as a substrate. Four independent transformants were assayed for each pair of constructs, and the numbers indicate the *LacZ* activity in Miller unit. The error bars indicate standard errors. (C) Bimolecular fluorescence complementation assay (BiFC). The interaction between MAP3K16 and MKK3 was examined by BiFC as described in the Materials and Methods. Protoplasts, which were prepared from tobacco (*N. benthamiana*) leaves infiltrated with pSPYNE-35S and pSPYCE-35S constructs, were observed under microscope.

interacted with the kinase domain alone albeit with lower intensity (Fig. 7A). The interaction between the full-length MAP3K16 and ABR1 was confirmed by pulldown assays (Fig. 7B), in which *in vitro* translated MAP3K16 was retained by MBP (maltose-binding protein)-tagged ABR1 (Fig. 7B, lane 2) but not by MBP alone (Fig. 7B, lane 1). In addition, BiFC assays were performed to further confirm the MAP3K16-ABR1 interaction (Fig. 7C). In the assay, fluorescence signals, which appeared as a single broad spot in the cell, were observed in tobacco cells infiltrated with *Agrobacteria* harboring the YFP^N-MAP3K16 and the YFP^C-ABR1 constructs.

Once confirmed the interaction between the full-length MAP3K16 and ABR1, we performed a deletion study to map the interaction domain of ABR1. Various ABR1 deletion constructs shown in Figs. 7D and 7E were prepared, and their interactions with the full-length MAP3K16 were investigated by two-hybrid assay (Fig. 7F). Deletion of the N-terminal portion (amino acids 1-180) did not abolish the interaction, indicating that the remaining portion, i.e., fragment AP2C consisted of the AP2 domain (amino acids 181-260) and the C-terminal portion (amino acids 261-391) is sufficient for the interaction. On the other hand, the C-terminal deletion (amino acids 261-391) abolished the interaction, suggesting that it is essential for the interaction and that the remaining portion (i.e., fragment NAP2, amino acids 1-260) is not sufficient for the interaction. Although necessary, C-terminal portion alone could not interact with MAP3K16. In summary, the deletion analysis showed that both AP2 domain and the C-terminal portion of ABR1 are necessary for the interaction.

In vitro kinase activity of MAP3K16

To investigate the enzymatic activity of MAP3K16, we carried out *in vitro* kinase assays. We first determined whether MAP3K16 possessed kinase activity. Recombinant MAP3K16 proteins, full-length or a N-terminal partial fragment containing the kinase domain only, were prepared as described in Materials and Methods. Their phosphorylation activity was then determined employing myelin basic protein (MyBP) as a substrate. Figure 8A shows that the full-length MAP3K16 could phosphorylate MyBP (lanes 1, 2). The partial fragment consisted of the MAP3K16 kinase domain (amino acids 1-263) also could phosphorylate MyBP (lanes 3, 4). Compared with the full-length protein, the partial fragment, which is considered to be a constitutively active form (Rodriguez et al., 2010), exhibited much higher phosphorylation activity.

Next, we investigated whether MAP3K16 could phosphorylate ABR1. In the above assay to examine MyBP phosphorylation, recombinant ABR1 was also phosphorylated by the constitutive active form (i.e., the kinase domain-containing fragment) of MAP3K16 (Fig. 8A, lane 4), when it was added to the reaction mixture with MyBP. In a separate assay employing ABR1 as an only substrate, ABR1 was phosphorylated by MAP3K16 (Fig. 8B, lanes 3, 4). Thus, our results indicate that the constitutive active form of MAP3K16 could phosphorylate ABR1 *in vitro*. Similarly, we also examined whether MAP3K16 could phosphorylate MKK3. Recombinant MKK3 protein was prepared as described in Materials and Method, and kinase assays were carried out. The result showed that MAP3K16 could phosphorylate MKK3 (Fig. 8C, lane 3). The constitutively active form of MAP3K16 may be lacking the putative regulatory domain (Rodriguez et al., 2010) and, consequently, may have lost its substrate specificity. To address the question, we examined the phosphorylation of several other MKKs, and the result showed that MKK3 was preferentially

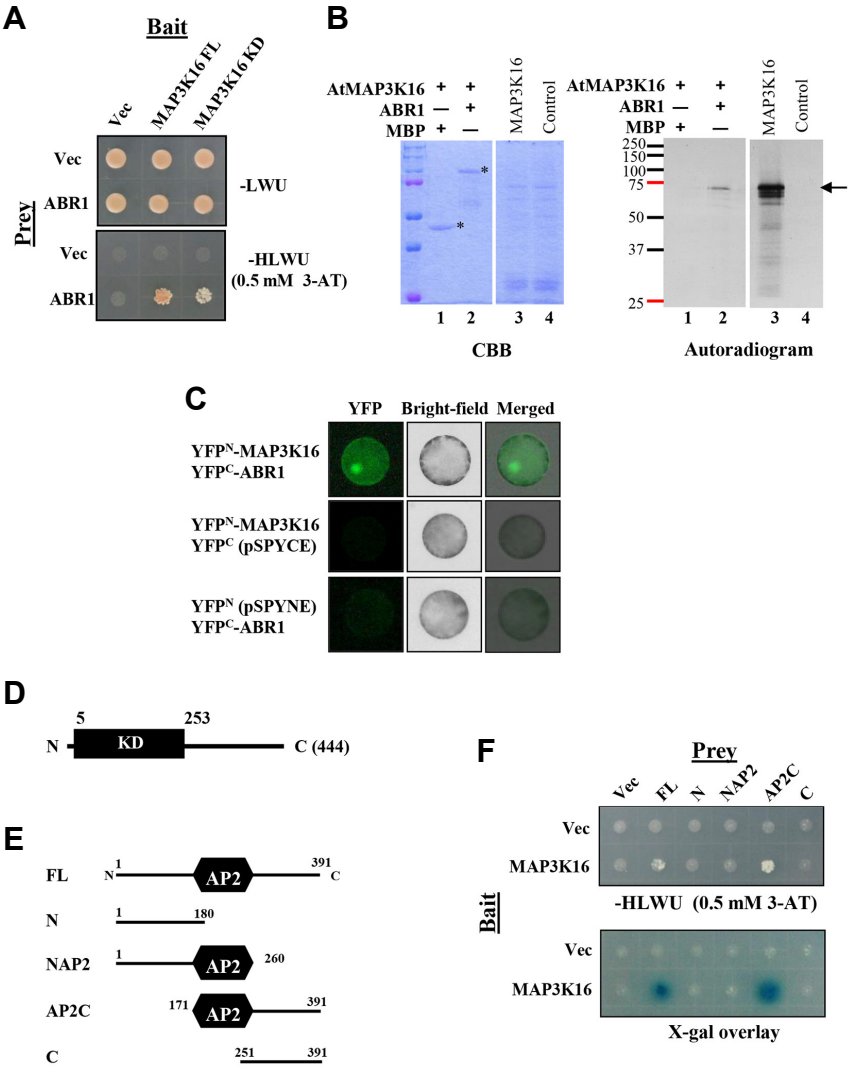

Fig. 7. Interaction of MAP3K16 with ABR1. (A) The interaction between MAP3K16 and ABR1 was investigated by two-hybrid assay, using ABR1 as bait and MAP3K16 as prey. FL, full-length. KD, kinase domain. (B) MBP (maltose binding protein) pulldown assay was performed using MBP-tagged ABR1 and *in vitro*-translated MAP3K16 labeled with ^{35}S. Lane 1, MBP only. Lane 2, MBP-ABR1. Lane 3, *in vitro* translation product of MAP3K16. Lane 4, negative control for *in vitro* translation. (C) Bimolecular fluorescence complementation assay (BiFC). The interaction between MAP3K16 and ABR1 was investigated by BiFC, as described in the "Materials and Methods". Protoplasts prepared from tobacco (*N. benthamiana*) leaves infiltrated with the pSPYNE-35S and pSPYCE-35S constructs pair were observed under microscope. (D) Schematic diagram of MA3K16 domain structure. The numbers indicate amino acid position. (E) Schematic diagram of ABR1 domain structure and the various fragments used in the two-hybrid assay in (F). The numbers indicate the amino acid position. (F) Two-hybrid assay to determine the interaction domains of ABR1 shown in (E). Full-length MA3K16 was used as bait, and various portions of ABR1 as prey. Transformants were grown on SC-HLWU plates containing 0.5 mM 3-aminotriazole (3-AT), and the *LacZ* reporter activity was determine by X-gal overlay assay.

phosphorylated by the active form of MAP3K16 (Supplementary Fig. S6).

DISCUSSION

The primary goal of our current study is to find out MAP3Ks that are involved in ABA and stress responses. Toward the end, we searched database and chose MAP3K16 and several other ABA- or salt-inducible MAP3Ks for functional analyses.

In our transgenic analyses, overexpression of *MAP3K16* conferred partial ABA insensitivity during early seedling growth stage and the susceptibility to water-deficit condition. On the other hand, the *MAP3K16* KO line displayed opposite phenotypes, notably, the ABA hypersensitivity during early seedling growth. The degree of hypersensitivity, however, was low probably because of the functional redundancy discussed below.

ABA affects several aspects of plant growth and development (Finkelstein, 2013), such as seed germination, seedling establishment (i.e., cotyledon greening/expansion and onset of vegetative growth) and subsequent postgermination growth, stress tolerance, and seed dormancy. Although ABA generally plays an inhibitory role during germination and postgermination growth, it inhibits postgermination seedling growth more efficiently than the germination process (Lopez-Molina et al., 2001). The ABA insensitivity of the *MAP3K16* OX lines was observed at this stage, and seed germination was not affected (Supplementary Fig. S1). In contrast, primary root elongation of transgenic seedlings was slightly hypersensitive to ABA inhibition (Fig. 2F), suggesting that *MAP3K16* OX phenotypes are developmental stage-dependent. Another noticeable ABA-associated phenotype of the *MAP3K16* OX lines was the susceptibility to water deficit, which may result from higher transpiration rates (Figs. 3D-3F). The reduced water-deficit tolerance is consistent with the ABA insensitivity observed at the seedling establishment stage.

Our transgenic analyses of other salt-inducible MAP3Ks (summarized in the Supplementary Table S1), MAP3K14/15/

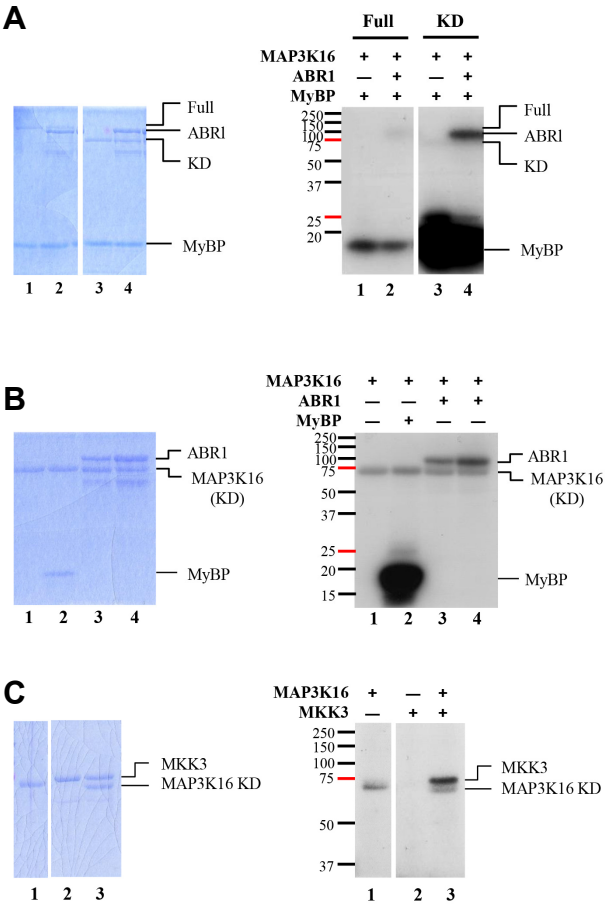

Fig. 8. Kinase activity of MAP3K16. (A) *In vitro* assay to investigate the kinase activity of MAP3K16. Recombinant MAP3K16 protein (~ 0.5 μg) tagged with maltose-binding protein was employed in an assay in which myelin basic protein (MyBP) was used as a substrate. The right panel shows an autoradiogram, and the left panel shows a gel stained with coomassie brilliant blue R (CBB). The same amount of MyBP (~ 1 μg) was used in lanes 1-4. In lanes 2 and 4, recombinant ABR1 (~1 μg) was also added as a substrate. (B) Phosphorylation of ABR1 by MAP3K16. *In vitro* kinase assay was carried out to study phosphorylation of ABR1 by MAP3K16 (kinase domain, KD). Approximately 1 μg of MAP3K16 was used, and the amount of ABR1 in lanes 3 and 4 was 0.8 μg and 1.6 μg, respectively. Left panel, CBB-stained gel. Right panel, autordiogram. The X-ray film exposure time was longer (~2. 5 times) than in (A). (C) Phosphorylation of MKK3 by MAP3K16 (kinase domain) was investigated by *in vitro* kinase assay. Assays were performed as in (A) and (B). Left panel, CBB-stained gel. Right panel, autoradiogram. The numbers in the autoradiograms indicate the position of size markers. The assay components in each reaction mixture are indicated above the autoradiograms in (A), (B), and (C).

17/18, indicate that they are likely to play similar roles to MAP3K16 in ABA and stress responses. The OX lines of the genes were ABA-insensitive during seedling establishment (i.e., cotyledon greening/expansion) stage and susceptible to water deficit (Fig. 5 and Supplementary Fig. S3). Like *MAP3K16* OX lines, the OX lines exhibited weak ABA-insensitivity during germination and weak ABA-hypersensitivity during root growth. Additionally, their KO lines exhibited similar phenotypes to those of the *MA3K16 KO* line (Supplementary Table S1). High degree of functional redundancy is, therefore, expected among the salt-inducible Arabidopsis MAP3Ks, and the weak KO phenotypes of *MAP3K16* and *MAP3K14/15/17/18* may be due to this functional redundancy.

It is noteworthy that the results of our transgenic analyses suggest the negative regulatory role of MAP3K14/15/16/17/18 in ABA response. The conclusion is based on our observation of OX phenotypes and the phenotypes of single KO lines without complementation analyses. Thus, the results must be interpreted with caution. Nonetheless, most distinct OX phenotypes (i.e., ABA insensitivity during seedling establishment stage and drought susceptibility) were observed with all OX lines (Supplementary Table S1), and opposite and complementary phenotypes were observed with their respective KO lines. Collectively, the results strongly support the conclusion that MAP3K14/15/16/17/18 play mainly negative regulatory roles in ABA response.

Recombinant MAP3K16 protein possesses kinase activity (Fig. 8), and, in an effort to identify putative MKK substrates, we found out that it interacts with MKK3 (Fig. 6, Supplementary Fig. S4). Consistent with this observation, recombinant MKK3 was phosphorylated by MAP3K16 *in vitro* (Fig. 8C). It remains to be determined whether MKK3 is phosphorylated by MAP3K16 *in vivo*. Nonetheless, the result suggests that MAP3K16 may function *via* the MAP kinase pathway reported by Danquah et al. (2015) (see below). They showed that MAP3K17/18 mediate ABA response by the MAP3K17/18-MKK3-MPK1/2/7/14 pathway. We also observed the MAP317 interaction with MKK3 (Supplementary Fig. S5A), although the MAP3K18 interaction with MKK3 was not observed presumably because of the lower sensitivity of our two-hybrid assay system.

Our results suggest that ABR1 may also be a substrate of MAP3K16. ABR1 was isolated as one of the positive clones in the two-hybrid screen to isolate MAP3K16-interacting proteins. Additionally, recombinant ABR1 was phosphorylated by MAP3K16 *in vitro* (Figs. 8A and 8B). As in the above case of MKK3, it remains to be determined whether ABR1 is a MAP3K16 substrate *in planta*. However, it is noteworthy that ABR1 is one of the few negative regulators of ABA response (Pandey et al., 2005) and that MAP3K16 plays mainly a negative regulatory role. In line with the notion that ABR1 may be an *in vivo* substrate of MAP3K16, several genes (*COR15A*, *COR47*, *RAB18*, *RD29A*, *RD22*, and *RD29A*) that are up-regulated in the *abr1* mutant were found to be down-regulated in the *MAP3K16* OX lines in our limited analysis of gene expression changes (Supplementary Fig. S7). There is a precedent in which a MAP3K phosphorylates a substrate other than MKKs. For instance, Arabidopsis MAP3K CTR1 phosphorylates EIN2 (Ju et al., 2012; Qiao et al., 2012) as well as MKK9 (Yoo et al., 2008).

While our work is in progress, the function of MAP3K17 and MAP3K18 has been reported. According to Danquah et al. (2015), MAP3K17/18 activate MKK3, which in turn acti-

vates MPK1/2/7/14. The MAPK cascade is activated by the core ABA signaling module, and the *mkk3* and the *map3k17map3k18* mutants are ABA-hypersensitive. These mutant phenotypes are consistent with the *map3k16* phenotypes we observed. Matsuoka et al. (2015) reported similar results (i.e., MAP3K18-MKK3-MPK1/2/7 pathway) and showed that MAP3K18 is involved in leaf senescence process. Mitula et al. (2015), on the other hand, reported that MAP3K18 affects ABA sensitivity and stomatal index. Additionally, they showed that ABI1 regulates the MAP3K18 activity by promoting proteasomal degradation of MAP3K18.

In summary, our study demonstrated that MAP3K16 functions mainly as a negative regulator of ABA response during early seedling growth and in water-deficit response, although it plays a positive role in the regulation of root growth. MAP3K16 possesses a kinase activity and could phosphorylate ABR1, a negative regulator of ABA response. MAP3K16 also interacts with MKK3 and phosphorylate it *in vitro,* suggesting that, like MAP3K17/18, it may also function in the MKK3-MPK1/2/7/14 pathway. Other salt-inducible *MAP3Ks*, *MAP3K14/15/17/18*, exhibited OX and KO phenotypes similar to those of *MAP3K16*, suggesting that they may play similar roles in ABA response.

Note: Supplementary information is available on the Molecules and Cells website (www.molcells.org).

ACKNOWLEDGMENTS

This work was supported in part by the Basic Science Researcher Program through NRF grant (No. 2014R1A1A 2056798 to SYK) funded by the MOE and the Mid-career Researcher Program through NRF grant (No. 2011-0015455 to SYK) funded by the MEST, Republic of Korea. The authors are grateful to the Kumho Life Science Laboratory of Chonnam National University for providing equipment and plant growth facilities.

REFERENCES

Asai, T., Tena, G., Plotnikova, J., Willmann, M.R., Chiu, W.L., Gomez-Gomez, L., Boller, T., Ausubel, F.M., and Sheen, J. (2002). MAP kinase signalling cascade in Arabidopsis innate immunity. Nature *415*, 977-983.

Bechtold, N., and Pelletier, G. (1998). In planta Agrobacterium-mediated transformation of adult Arabidopsis thaliana plants by vacuum infiltration. Methods in Mol. Biol. *82*, 259-266.

Choi, H., Hong, J., Ha, J., Kang, J., and Kim, S.Y. (2000). ABFs, a family of ABA-responsive element binding factors. J. Biol. Chem. *275*, 1723-1730.

Choi, H.I., Park, H.J., Park, J.H., Kim, S., Im, M.Y., Seo, H.H., Kim, Y.W., Hwang, I., and Kim, S.Y. (2005). Arabidopsis calcium-dependent protein kinase AtCPK32 interacts with ABF4, a transcriptional regulator of abscisic acid-responsive gene expression, and modulates its activity. Plant Physiol. *139*, 1750-1761.

Colcombet, J., and Hirt, H. (2008). Arabidopsis MAPKs: a complex signalling network involved in multiple biological processes. Biochem. J. *413*, 217-226.

Cutler, S.R., Rodriguez, P.L., Finkelstein, R.R., and Abrams, S.R. (2010). Abscisic acid: emergence of a core signaling network. Annu. Rev. Plant Biol. *61*, 651-679.

Czechowski, T., Stitt, M., Altmann, T., Udvardi. M.K., and Scheible, W.R. (2005). Genome-wide identification and testing of superior reference genes for transcript normalization in Arabidopsis. Plant Physiol. *139*, 5-17.

Danquah, A., de Zelicourt, A., Colcombet, J., and Hirt, H. (2014). The role of ABA and MAPK signaling pathways in plant abiotic stress responses. Biotechnol. Adv. *32*, 40-52.

Danquah, A., de Zelicourt, A., Boudsocq, M., Neubauer, J., Frei Dit Frey, N., Leonhardt, N., Pateyron, S., Gwinner, F., Tamby, J.P., Ortiz-Masia, D., et al. (2015). Identification and characterization of an ABA-activated MAP kinase cascade in Arabidopsis thaliana. Plant J. *82*, 232-244.

Duttweiler, H.M. (1996). A highly sensitive and non-lethal beta-galactosidase plate assay for yeast. Trends Genet. *12*, 340-341.

Finkelstein, R. (2013). Abscisic Acid synthesis and response. The Arabidopsis book / American Society of Plant Biologists *11*, e0166.

Fujii, H., and Zhu, J.K. (2009) Arabidopsis mutant deficient in 3 abscisic acid-activated protein kinases reveals critical roles in growth, reproduction, and stress. Proc. Natl. Acad. Sci. USA *106*, 8380-8385.

Fujii, H., Chinnusamy, V., Rodrigues, A., Rubio, S., Antoni, R., Park, S.Y., Cutler, S.R., Sheen, J., Rodriguez, P.L., and Zhu, J.K. (2009). In vitro reconstitution of an abscisic acid signalling pathway. Nature *462*, 660-664.

Fujita, Y., Nakashima, K., Yoshida, T., Katagiri, T., Kidokoro, S., Kanamori, N., Umezawa, T., Fujita, M., Maruyama, K., Ishiyama, K., et al. (2009). Three SnRK2 protein kinases are the main positive regulators of abscisic acid signaling in response to water stress in Arabidopsis. Plant Cell Physiol. *50*, 2123-2132.

Fujita, Y., Fujita, M., Shinozaki, K., and Yamaguchi-Shinozaki, K. (2011). ABA-mediated transcriptional regulation in response to osmotic stress in plants. J. Plant Res. *124*, 509-525.

Holdsworth, M.J., Bentsink, L., and Soppe, W.J. (2008) Molecular networks regulating Arabidopsis seed maturation, after-ripening, dormancy and germination. New Phytol. *179*, 33-54.

Ichimura, K., Shinozaki, K., Tena, G., Sheen, J., Henry, Y., Champion, A., Kreis, M., Zhang, S., Hirt, H., Wilson, C., et al. (2002). Mitogen-activated protein kinase cascades in plants: a new nomenclature. Trends Plant Sci. *7*, 301-308.

Jammes, F., Song, C., Shin, D., Munemasa, S., Takeda, K., Gu, D., Cho, D., Lee, S., Giordo, R., Sritubtim, S., et al. (2009). MAP kinases MPK9 and MPK12 are preferentially expressed in guard cells and positively regulate ROS-mediated ABA signaling. Proc. Natl. Acad. Sci. USA *106*, 20520-20525.

Jefferson, R.A., Kavanagh, T.A., and Bevan, M.W. (1987) GUS fusions: β-glucuronidase as a sensitive and versatile gene fusion marker in higher plants. EMBO J. *20*, 3901-3907.

Ju, C., Yoon, G.M., Shemansky, J.M., Lin, D.Y., Ying, Z.I., Chang, J., Garrett, W.M., Kessenbrock, M., Groth, G., Tucker, M.L., et al. (2012). CTR1 phosphorylates the central regulator EIN2 to control ethylene hormone signaling from the ER membrane to the nucleus in Arabidopsis. Proc. Natl. Acad. Sci. USA *109*, 19486-19491.

Kang, J.Y., Choi, H.I., Im, M.Y., and Kim, S.Y. (2002). Arabidopsis basic leucine zipper proteins that mediate stress-responsive abscisic acid signaling. Plant Cell *14*, 343-357.

Khokon, M.A., Salam, M.A., Jammes, F., Ye, W., Hossain, M.A., Uraji, M., Nakamura, Y., Mori, I.C., Kwak, J.M., and Murata, Y. (2015). Two guard cell mitogen-activated protein kinases, MPK9 and MPK12, function in methyl jasmonate-induced stomatal closure in Arabidopsis thaliana. Plant Biol. *17*, 946-952.

Kim, T.H., Bohmer, M., Hu, H., Nishimura, N., and Schroeder, J.I. (2010). Guard cell signal transduction network: advances in understanding abscisic acid, CO2, and Ca^{2+} signaling. Annu. Rev.

Plant Biol. *61*, 561-591.

Lampard, G.R., Lukowitz, W., Ellis, B.E., and Bergmann, D.C. (2009). Novel and expanded roles for MAPK signaling in Arabidopsis stomatal cell fate revealed by cell type-specific manipulations. Plant Cell *21*, 3506-3517.

Lee, S.J., Cho, D.I., Kang, J.Y., and Kim, S.Y. (2009). An ARIA-interacting AP2 domain protein is a novel component of ABA signaling. Mol. Cells *27*, 409-416.

Lee, S.J., Lee, M.H., Kim, J.I., and Kim, S.Y. (2015). Arabidopsis putative MAP kinase kinase kinases Raf10 and Raf11 are positive regulators of seed dormancy and ABA response. Plant Cell Physiol. *56*, 84-97.

Liu, Y. (2012). Roles of mitogen-activated protein kinase cascades in ABA signaling. Plant Cell Rep. *31*, 1-12.

Lopez-Molina, L., Mongrand, S., and Chua, N.H. (2001). A postgermination developmental arrest checkpoint is mediated by abscisic acid and requires the ABI5 transcription factor in Arabidopsis. Proc. Natl. Acad. Sci. USA *98*, 4782-4787.

Ma, Y., Szostkiewicz, I., Korte, A., Moes, D., Yang, Y., Christmann, A., and Grill, E. (2009). Regulators of PP2C phosphatase activity function as abscisic acid sensors. Science *324*, 1064-1068.

Matsuoka, D., Yasufuku, T., Furuya, T., and Nanmori, T. (2015). An abscisic acid inducible Arabidopsis MAPKKK, MAPKKK18 regulates leaf senescence via its kinase activity. Plant Mol. Biol. *87*, 565-575.

Mitula, F., Tajdel, M., Ciesla, A., Kasprowicz-Maluski, A., Kulik, A., Babula-Skowronska, D., Michalak, M., Dobrowolska, G., Sadowski, J., and Ludwików, A. (2015). Arabidopsis ABA-activated kinase MAPKKK18 is regulated by Protein phosphatase 2C ABI1 and the ubiquitin-proteasome pathway. Plant Cell Physiol. *56*, 2351-2367.

Nambara, E., and Marion-Poll, A. (2005). Abscisic acid biosynthesis and catabolism. Annu. Rev. Plant Biol. *56*, 165-185.

Pandey, G.K., Grant, J.J., Cheong, Y.H., Kim, B.G., Li, L. and Luan, S. (2005). ABR1, an APETALA2-domain transcription factor that functions as a repressor of ABA response in Arabidopsis. Plant Physiol. *139*, 1185-1193.

Park, S.Y., Fung, P., Nishimura, N., Jensen, D.R., Fujii, H., Zhao, Y., et al. (2009). Abscisic acid inhibits type 2C protein phosphatases via the PYR/PYL family of START proteins. Science *324*, 1068-1071.

Qiao, H., Shen, Z., Huang, S.S., Schmitz, R.J., Urich, M.A., Briggs, S.P., and Ecker, J.R. (2012). Processing and subcellular trafficking of ER-tethered EIN2 control response to ethylene gas. Science *338*, 390-393.

Rodriguez, M.C., Petersen, M., and Mundy, J. (2010). Mitogen-activated protein kinase signaling in plants. Annu. Rev. Plant Biol. *61*, 621-649.

Takahashi, Y., Soyano, T., Kosetsu, K., Sasabe, M., and Machida, Y. (2010). HINKEL kinesin, ANP MAPKKKs and MKK6/ANQ MAPKK, which phosphorylates and activates MPK4 MAPK, constitute a pathway that is required for cytokinesis in Arabidopsis thaliana. Plant Cell Physiol. *51*, 1766-1776.

Teige, M., Scheikl, E., Eulgem, T., Doczi, F., Ichimura, K., Shinozaki, K., Dangl, J.L., and Hirt, H. (2004). The MKK2 pathway mediates cold and salt stress signaling in Arabidopsis. Mol. Cell *15*, 141-152.

Walter, M., Chaban, C., Schütze, K., Batistic, O., Weckermann. K., Näke, C., Blazevic, D., Grefen, C., Schumacher, K., Oecking, C., et al. (2004). Visualization of protein interactions in living plant cells using bimolecular fluorescence complementation. Plant J. *40*, 428-438.

Xing, Y., Jia, W.S., and Zhangl, J.H. (2008). AtMKK1 mediates ABA-induced CAT1 expression and H2O2 production via AtMPK6-coupled signaling in Arabidopsis. Plant J. *54*, 440-451.

Xing, Y., Jia, W.S., and Zhang, J.H. (2009). AtMKK1 and AtMPK6 are involved in abscisic acid and sugar signaling in Arabidopsis seed germination. Plant Mol. Biol. *70*, 725-736.

Xiong, L.M., Schumaker, K.S., and Zhu, J.K. (2002). Cell signaling during cold, drought, and salt stress. Plant Cell *14*, S165-S183.

Yoo, S.D., Cho, Y.H., and Sheen, J. (2007). Arabidopsis mesophyll protoplasts: a versatile cell system for transient gene expression analysis. Nat. Protoc. *2*, 1565-1572.

Yoo, S.D., Cho, Y.H., Tena, G., Xiong, Y., and Sheen, J. (2008). Dual control of nuclear EIN3 by bifurcate MAPK cascades in C2H4 signalling. Nature *451*, 789-795.

Yoshida, T., Mogami, J., and Yamaguchi-Shinozaki, K. (2015). Omics approaches toward defining the comprehensive abscisic acid signaling network in plants. Plant Cell Physiol. *56,* 1043-1052.